32nd Annual International Conference of the IEEE EMBS
Buenos Aires, Argentina, August 31 - September 4, 2010

Detection of Exudates in Retinal Images Using a Pure Splitting Technique

Hussain F. Jaafar, Asoke K. Nandi, and Waleed Al-Nuaimy

Abstract— **Diabetic retinopathy is a major cause of blindness. Earliest signs of diabetic retinopathy are damage to blood vessels in the eye and then the formation of lesions in the retina. This paper presents an automated method for the detection of bright lesions (exudates) in retinal images. In this work, an adaptive thresholding based on a novel algorithm for pure splitting of the image is proposed. A coarse segmentation based on the calculation of a local variation for all image pixels is used to outline the boundaries of all candidates which have clear borders. A morphological operation is used to refine the adaptive thresholding results based on the coarse segmentation results. Using a clinician reference standard (ground truth), images with exudates were detected with 91.2% sensitivity, 99.3% specificity, and 99.5% accuracy. Due to its results the proposed method can achieve superior performance compared to existing techniques and is robust to image quality variability.**

I. Introduction

Early detection of diabetic retinopathy (DR) is very helpful for the protection of visual loss. Exudates are one of the most prevalent lesions in the early stages of DR. In addition, they represent the specific marker for the existence of co-existent retinal oedema, the major cause of visual loss. They are lipid leaks from blood vessels of abnormal retinas [1]. Detection of exudates by ophthalmologists is a laborious process as they have to spend a great deal of time in manual analysis and diagnosis. Moreover, manual detection requires using chemical dilation material which takes time and has negative side effects on patients. Hence automated screening techniques for exudate detection have great significance in saving costs, time, and labour in addition to avoiding the side effects on patients. Colour fundus images are used to detect exudates in retinal images and to establish their location, size, and severity grade.

Several techniques for the detection of exudates have been proposed. Notable amongst these are those utilising fuzzy C-means for segmentation in the different classification methods [2]–[4]. Sopharak *et al.* [2] utilised morphological techniques for fine-tuning. However, this method sometimes detects bright artifacts wrongly as exudates. Osareh *et al.* [3] used artificial neural network to classify segmented regions at lesion based classification. The method works well, but the detection accuracy in case of uneven illumination is low. Kande *et al.* [4] used spatial neighborhood information into the standard FCM clustering for exudate classification.

Manuscript received April 1, 2010. This work was supported by the Iraqi government / Ministry of Higher Education and Scientific Research.

Hussain F. Jaafar , Asoke K. Nandi and Waleed Al-Nuaimy are with the Department of Electrical Engineering and Electronics, University of Liverpool, Brownlow Hill, Liverpool, L69 3GJ, UK, (e-mails: h.jaafar, a.nandi, wax @liverpool.ac.uk).

Many other techniques have been proposed [5]–[7]. Welfer *et al* [5] proposed a new method based on mathematical morphology for detecting exudates. The drawback of this approach is that it produces high misclassified portion for images that do not contain exudates. Garcia *et al.* [6] investigated three neural network classifiers multilayer perceptron, radial basis function, and support vector machine for the detection of exudates. Sopharak *et al.* [7] employed naive Bayes and support vector machine classifiers for feature selection and classification of exudates. The method achieved good performance measures, but both classifiers occasionally miss faint exudates.

This paper describes an automated method for exudate detection in retinal images using an adaptive thresholding and image partitioning. A pure splitting algorithm is used to split the image into a number of homogeneous sub-images depending on the image uniformity. A statistical hypothesis test based on image features, such as mean and variance values is used to test the homogeneity of the entire image and resulting sub-images. A sequence of splitting operations for the whole image and then new sub-images can be regarded depending on the results of homogeneity tests.

A coarse segmentation based on calculating a local variation of all pixels of the image is used to outline the boundaries of all adaptive thresholding candidates which have clear borders. A morphological operation is used to combine of the coarse segmentation and adaptive thresholding results for final exudate detection.

II. Methedology

First of all, all colour images are initially resized to one of the common standard sizes as 640×480 pixels so that the proposed method could be applied to different databases easily. As stated by Walter *et al.* [8], the exudates appear more contrasted in the green channel component than the other channels of the colour image. Hence, the green channel component images are used, in our method, to detect exudate by four steps: pre-processing using shade correction, smoothing, and optic disk elimination (Section A), adaptive thresholding using a pure splitting algorithm and histogram-based thresholding (Section B), coarse segmentation based on calculating a local variation of all image pixels (Section C), and final exudate detection by combining of the adaptive thresholding and coarse segmentation results (Section D).

A. Pre-processing

Due to variability in the acquisition process and physical features of a patient, such as skin and iris colour, most of the retinal images are uneven illuminated. This problem affects

seriously the processes of automatic detection of bright lesions and makes it difficult to distinguish exudates from other bright features in images. So shade correction and noise removal are crucial tasks to prepare images for post-processing. To correct uneven illumination of images, a morphological top-hat operator with disk-shaped structuring element and fixed radius of 20 pixels was applied to the green component of the colour image. To reduce noise, a 3×3 median filter is applied to the shade corrected image.

The bright optic disk can appear with similar features as exudates, and it is often identified incorrectly as an exudate; so it is essential to eliminate it before exudate detection steps. Thus, the method described by Sekhar *et al.* [9] has been followed to determine the centre and the radius of the optic disk. In this method, a circular region of interest is found by isolating the brightest region of the image using morphological operations, and then the Hough transform is used to detect the main circular feature within the positive horizontal gradient image in this region of interest. The estimated location of optic disk is masked with a circular disk of colour equal to the average intensity of the image.

B. Adaptive Thresholding

Fast segmentation of the image can be performed using global thresholding, but it mostly results in undesired binary results especially when the input images are uneven or of poor quality. Consequently, adaptive local thresholding methods are used to get better segmentation results. However these methods have the disadvantage of slow running speed due to the re-computing operation of threshold value to each local region. In this paper the adaptive thresholding is based on a combination of global and local thresholding. Local thresholding is applied on non-uniform background images by partitioning the image into uniform sub-images. The number of the sub-images depends on image uniformity and brightness distribution throughout the image. Global thresholding is then applied to each uniform sub-image using histogram-based thresholding.

This stage consists of two steps: first step is to investigate the optimal number of image partitions using a pure splitting algorithm. The second stage is to apply a global thresholding to each sub-image using a histogram-based thresholding.

1) Pure Splitting Algorithm: Retinal images, like most medical images, are so complex that they cannot be segmented with a single threshold. With such concern, it is suitable to use region-based segmentation. Region-based segmentation algorithms are classified into three schemes: pure merging, pure splitting, and split-and-merge [10]. In the first scheme the image is divided into small regions which are then merged to form larger regions under a homogeneity criterion. The pure splitting methods perform segmentation of the entire image and then successively split each segment into quarters until the homogeneity is reached. Split-and-merge scheme is based on partitioning the image into square sub-regions until homogeneity is verified. Then a merging process is applied to neighbouring sub-regions that satisfy a uniformity criterion. In the proposed method, we employ the pure splitting technique. Lee [11] applied the pure splitting method by viewing the entire image as initial segmentation. This entire image is segmented into quarters if it is not homogeneous, then each new segment is successively segmented into quarters if it is not homogeneous enough.

The proposed method follows the same procedures in [11], but with essential difference in the number of segmented regions. It successively subdivides each current segment, if it is not homogeneous enough, into two equal segments. In subdividing the non-homogeneous segment into two parts instead of four quarters, our aim is to avoid merging operations which may be required in the case of four quarters. As a result, the number of homogeneous sub-images may be less than that of four quarters and hence it is faster computationally. Homogeneity of the sub-image is tested using statistical hypothesis test and parameters from the image characteristics. The characteristic features of the image are used to provide those parameters which serve as constraints in the statistical hypothesis test. In this stage the green channel of the colour image is used after optic disk elimination, blood vessels removal, excluding the dark background around the retina and smoothing. In this method a region of arbitrary size is tested for the homogeneity.

To perform homogeneity test, the region is assumed as two-dimensional random field. The random field is divided into two parts as two sets of random variables: X_i with mean m_1 and variance σ_1 and Y_j with mean m_2 and variance σ_2. The means test is defined as: the absolute difference of the intensities summation of X_i and Y_j is less than a threshold (ε). If the mean test is valid, the variances test is then performed using the likelihood ratio test to test the hypothesis H_0: $\sigma_1=\sigma_2$. Homogeneity test is right as long as the hypothesis H_0 is valid. Otherwise, the region is not homogeneous. If any region is not homogeneous, then it is further subdivided into two equal regions.

2) Histogram-based Thresholding: Although they are fast and simple approaches for the image segmentation, global thresholding methods mostly fail when the background is uneven illuminated. Two methods have been used to rectify this problem [10]: first by applying the global thresholding to uniform local sub-images, and second by recursive application of the global method to increasingly fine-gained regions. In our method the uniform illumination locality is achieved by partitioning the image into homogeneous sub-images. Hence, these sub-images are easy to be segmented by any global thresholding methods such as histogram-based thresholding. As pixel intensities of homogeneous image are clustered around two groups, its histogram will be bi-modal.

Based on the result of image splitting gained in the preceding step, histogram-based thresholding was applied to the locations of sub-images of the smoothed green component channel (G_s) to obtain the segmentation of the image. Let a partition (P) of the image is defined as a subset of G_s with respect to uniform lighting criterion. Hence running a global thresholding (T) throughout the image with variable threshold values (α) depending on the individuality of each sub-image can be represented by G_1 as in Eq. (1);

$$G_1 = \sum_{l \in k} T_{\alpha_l}(P_l) \tag{1}$$

where k is the number of sub-images.

C. Coarse Segmentation

Due to the acquisition process, very often retinal images contain light reflection regions with brightness similar as or more than exudates. However, most of the light reflection regions do not have clear boundaries, while most exudates have clear margins in different degrees depending on the DR grade. One way to make use of this feature is to calculate the local variation for each pixel to get a standard deviation image. This image shows the main characterisation of the closely distributed clusters of exudates. Before applying the local variation operator, the high contrast blood vessels must be eliminated. Thus a morphological closing operator (ψ) was applied to the pre-processed image (G_p) with disk-shaped structuring element (ς_1) of radius 6 pixels. The resulting image is denoted by G_2 as in Eq. (2). The operation of local variation calculation can be formulated by Eq. (3), and resulting image is denoted by G_3;

$$G_2 = \psi^{\varsigma_1}(G_p) \tag{2}$$

$$G_3(x) = \frac{1}{N-1}\sum_{i \in w(x)} \left(G_2(i) - \mu(x)\right)^2 \tag{3}$$

where x is a set of all pixels in a sub-window $w(x)$, N is the number of pixels in $w(x)$, $\mu(x)$ is the mean value of $G_2(i)$ and $i \epsilon w(x)$. The selection of window size relies on the demanded compromise between sensitivity and precision values. Based on the experimental tests, we found the window size of 9×9 gives good results. To remove the objects, which have low local variation, from the standard deviation image, automatic thresholding using Otsu's method [12] was applied.

In order to classify non-exudates and then exclude them, the coarse segmented objects were discriminated using features such as major axis length, minor axis length, area, and solidity. These properties were utilised in such a way that some relations between them or some limits in their values can easily distinguish properties of non-exudates. One example of these properties is long and narrow areas which are formed due to bright vessels.

A morphological dilation operator (D), with a disk-shaped structuring element (ς_2) of radius 3 pixels, was applied on the segmented image to ensure that the majority of neighbouring pixels are included in the candidate regions. Then a morphological clear border operator (C) was applied to suppress structures that are lighter than their surrounding and connected to the image border. The coarse exudate detection result is denoted by G_4 as in Eq. (4);

$$G_4 = C\left(D^{\varsigma_2}[T_\alpha(G_3)]\right) \tag{4}$$

where T is a thresholding operator with automatic level (α).

D. Final Exudate detection

Due to light reflection and some bright blood vessels, the adaptive thresholding result often contains some non-exudates. Thus a combination of the coarse segmentation and adaptive thresholding images is used to improve the results. The final fine segmented image (G_5) is accomplished by applying a logical intersection operator on the coarse segmentation and adaptive thresholding results as in Eq. (5);

$$G_5 = G_1 \bigcap G_4 \tag{5}$$

The coarse segmented image outlines candidates of the adaptive thresholding result in such a way that only those candidates of clear border can be classified as exudates.

III. Results and Performance Evaluation

Experiments have been conducted to test and tune the proposed method and later evaluate the results versus clinician hand-labeled images. We used a set of 190 normal and abnormal images from different databases as follows:

- 89 images from the DIARETDB1 database [13]. 47 of them contain exudates while the remaining 42 either contain other type of lesions or are normal. 47 images, labeled by clinician in terms of lesions pixel by pixel, corresponding to exudative images are also available with this database.
- 50 abnormal images from the DIARETDB0 database with their corresponding images which are roughly marked by clinician with circles at lesion locations [14].
- 17 images with hard exudates and their clinician labeled images, in terms of lesions, from the Messidor database [8].
- 34 normal images from the Drive database [15].

The proposed method was tested and tuned using the 50 abnormal images from DIARETDB0 database and their corresponding clinician roughly marked images. 64 images (47 from DIARETDB1 and 17 from Messidor databases) with their clinician hand-labeled images were used to validate the proposed method in the pixel levels with 91.2%, 99.3%, 99.5% sensitivity, specificity, and accuracy respectively. To measure its ability to distinguish between normal and abnormal images, 123 images (34 images from Drive and 89 images from DIARETDB1 databases) were used to evaluate the proposed method at image-based classification, and the accuracy was 97.6%.

Performance of the proposed method was assessed quantitatively by comparing the results with clinician hand-labeled data. Four types of pixels are considered in the method evaluation: true positive (*TP*), false positive (*FP*), false negative (*FN*), and true negative (*TN*). These quantities were computed with each individual image to measure: *Sensitivity*=*TP*/(*TP*+*FN*), *Specificity*=*TN*/(*TN*+*FP*), and *Accuracy*=(*TP*+*TN*)/(*TP*+*FP*+*TN*+*FN*).

The proposed method has been adapted to deal with variable image quality through taking the individual image features into account. Image information, such as mean and variance values are computed and used to determine the requisite parameters for optimal pure splitting and then adaptive thresholding. The method employs a local variation operation to outline the boundaries of candidates, resulted by adaptive thresholding, in such a way that only candidates which have clear border are classified as exudates.

After visual inspection of the results and comparison of the performance of this technique, there appears to be a high level of false positives. While this is undesirable, it does not in our case result in false alarms. The reason for this is that

the misclassified pixels tend to lie in the immediate vicinity of true positives (surrounding small blobs), and the resulting interpretation of the images is therefore unaffected.

Table 1 shows a comparison between the performance measures of the proposed method and some related works using DIARETDB1 database. Table 2 shows a comparison between the performance measures of the proposed method and some distinctive related works with different databases.

TABLE 1
COMPARISON OF PERFORMANCES WITH DIARETDB1 DATABASE

Reference	Sens.%	Spec.%	Acc.%	Test set
Kande et al [4]	86	98	---	47
Welfer et al [5]	70.48	98.84	---	47
Proposed method	89.8	99.3	99.4	47

Sens. = Sensitivity, Spec. = Specificity, Acc. = Accuracy.

TABLE 2
COMPARISON OF PERFORMANCES WITH DEFERENT DATABASES

Reference	Sens.%	Spec.%	Acc.%	Test set
Osareh et al [3]	93	94.1	---	67
Garcia et al [6]	88.14	92.6	97	67
Sopharak et al [7]	92.28	98.52	98.41	39
Proposed method	91.2	99.3	99.5	64

Sens. = Sensitivity, Spec. = Specificity, Acc. = Accuracy.

Fig. 1 shows an input image, results of all stages including the final method result and the clinician ground truth result.

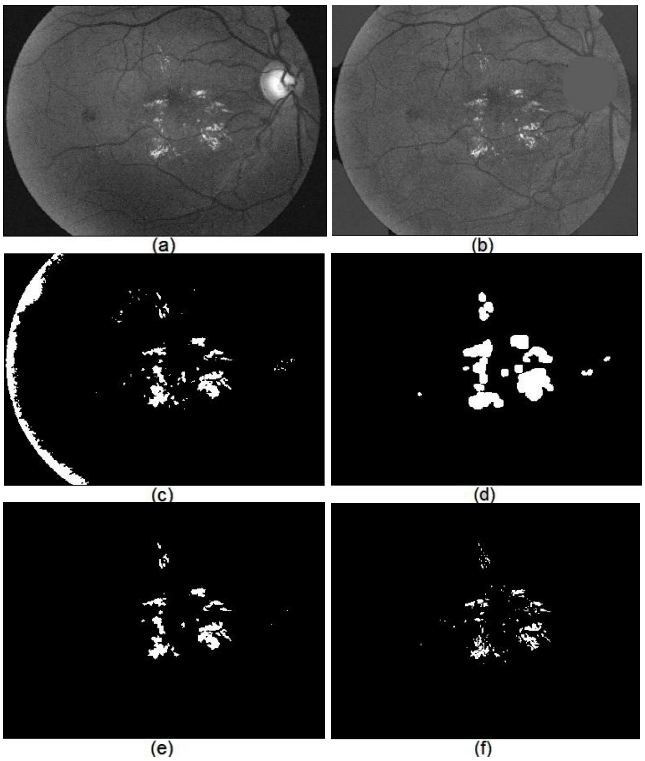

Fig.1. (a) Green channel component image. (b) Pre-processed image. (c) Result of the adaptive thresholding. (d) Result of the coarse segmentation. (e) Final exudate detection result. (f) Clinician hand-labeled result.

IV. CONCLUSIONS

The real challenge in creating automated exudates detection arises from wide differences in the illumination within a single image as well as among different images. Performance measures point to an improvement in the specificity and accuracy measures, as well as reasonable sensitivity measure compared with many other related works, namely the high performance method in [7]. Limitations in our work arise due to some incorrect non-exudates detection which are caused by those artifacts that have similar features of real exudates.

Finally, our algorithm is applicable to other problems of retinal images and easy to be expanded and developed for a better performance. Future work will address improvement of the performance measures by using domain knowledge of the blood vessels to rectify the problem of artifacts.

ACKNOWLEDGMENTS

The authors would like to thank DIARETDB1 [13] and DIARETDB0 [14] Database Center, the Center of Mathematical Morphology, France [8], and Drive Database Center [15] for the co-operation in providing retinal images.

REFERENCES

[1] D. E. Singer, D. M. Natham, H. A. Fogel, and A. P. Schachat, "Screening for diabetic retinopathy," *Ann. Intern. Med.*, vol. 116(8) pp. 660-671, 1992.

[2] A. Sopharak, and B. Uyyanonvara, "Automatic exudates detection from non-dilated diabetic retinopathy retinal images using fuzzy c-means clustering," *Sensor*, vol. 9(3), pp. 2148-2161, 2009.

[3] A. Osareh, M. Mirmehdi, B. Thomas, and R. Markham, "Automated identification of diabetic retinal exudates in digital colour images," *Ophthalmol*, vol. 87, pp. 1220-1223, 2003.

[4] G. Kande, P. Subbaiah, and T. Savithri, "Segmentation of exudates and optic disk in retinal images," *IEEE Sixth Indian Conference on Computer Vision, Graphic & Image Processing*, 2008.

[5] D. Welfer, J. Scharcanski, and D. R. Marinho, "A coarse-to-fine strategy for automatically detecting exudates in color eye fundus images," *Computerized Medical Imaging and Graphics*, 975, 2009.

[6] M. Garcia, C. I. Sanchez, M. I. Lopez, D. Abasolo, and R. Hornero, "Neural network basad detección of hard exudates in retinal images," *Computer Methods and Programs in Biomedicine*, 93, pp. 9-19, 2009.

[7] A. Sopharak, M. N. Dailey, B. Uyyanonvara, S. Barman, T. Williamson, K. T. Nwe, and Y. A. Moe, "Machine learning approach to automatic exudate detection in retinal images from diabetic retinopathy," *Journal of Modern Optics*, pp. 1-12, 2009.

[8] T. Walter, J. C. Klein, and P. Massin, "A Contribution of image processing to the diagnosis of diabetic retinopathy detection of exudates in colour fundus images of the human retina," *IEEE Trans. Med. Imaging*, 21, pp. 1236-43, 2002.

[9] S. Sekhar, W. Al-Nuaimy, and A. K. Nandi, "Automated localization of optic disk and fovea in retinal fundus images," *ISBI*, *France*, pp. 1577-1580, 2008.

[10] S. Chen, W. Lin, and C. Chen, "Split-and-merge image segmentation based on localized feature analysis and statistical test," *Graphical Models and Image Processing*, vol. 53(5), pp. 457-475, 1991.

[11] C. H. Lee, "recursive region splitting at hierarchical scope views," *Vision Graphics Image Process*., vol. 33, pp. 237-256, 1986.

[12] N. Otsu, "A Threshold Selection Method From Gray-Levels Histograms," *IEEE Trans. Systems, Man, and Cybernetics*, vol. 9(1), pp. 62-66, 1979.

[13] T. Kauppi, V. Kalesnykiene, J. K. Kamarainen, L. Lensu, I. Sorri, A. Raninen, R. Voutilainen, J. Pietila, H. Kalviainen, and H. Uusitalo, "the DIARETDB1 diabetic retinopathy database and evaluation protocol," *Technical report, Lappeenranta University of Technology and University of Kuopio, Finland*, 2007.

[14] T. Kauppi, V. Kalesnykiene, J. K. Kamarainen, L. Lensu, I. Sorri, H. Kalviainen, and J. Pietila, "DIARETDB0: Evaluation database and morphology for diabetic retinopathy algorithm," *Technical report*, Lappeenranta University of Technology, Finland, 2006.

[15] J. J. Staal, M. D. Abramoff, M. Niemeijer, M. A. Viergever, and B. van Ginneken, "Ridge based vessels segmentation in color images of the retina," *IEEE Transaction on Medical imaging*, vol. 23, pp. 501-509, 2004.